Pis'ma v ZhETF, vol.72, iss.5, pp.361 - 365

HIGH DENSITY PHENOMENA IN HYDROGEN PLASMA

V.S.Filinov[1)], *M.Bonitz*[+], *V.E.Fortov*

High Energy Density Research Center RAS, 127412 Moscow, Russia

[+]*Fachbereich Physik, Universität Rostock, D-18051 Rostock, Germany*

Submitted 27 June 2000

Resubmitted 1 August 2000

A novel path integral representation of the many-particle density operator is presented which makes direct Fermionic path integral Monte Carlo simulations feasible over a wide range of parameters. The method is applied to compute the pressure, energy and pair distribution functions of a hydrogen plasma in the region of strong coupling and strong degeneracy. Our numerical results allow to analyze atom and molecule formation and breakup and predict, at high density, proton ordering and pairing of electrons.

PACS: 52.25.Kn, 52.65.-y

Coulomb systems continue to attract the interest of researchers in many fields, including plasmas, astrophysics and solids, see Refs. [1, 2] for an overview. The most interesting phenomena such as metallic hydrogen, plasma phase transition, bound states, etc., occur in situations where the plasma is both strongly coupled and strongly degenerate. However, in this region, the thermodynamic properties of the plasma only poorly known. The need for the simultaneous account of strong Coulomb and quantum effects makes a theoretical treatment very difficult. Among the most promising theoretical approaches to these systems are path integral quantum Monte Carlo (PIMC) techniques, see e.g. [3, 4].

In this Letter we demonstrate that for many current problems in dense warm plasmas ($k_BT > 0.1\,\mathrm{Ry}$) direct PIMC simulations can, in fact, be carried out with acceptable efficiency. We report results for the internal energy, equation of state and pair distribution functions of partially ionized hydrogen in a wide range of coupling and degeneracy parameters, $\Gamma = (4\pi n_e/3)^{1/3}e^2/4\pi\epsilon_0 k_B T$ and $\chi = n_e\lambda_e^3$ (λ_e is the electron thermal wave length $\lambda_e^2 = 2\pi\hbar^2\beta/m_e$). Furthermore, our calculations predict, at high density, ordering of protons as well as pairing of electrons.

As is well known the thermodynamic properties of a quantum system are fully determined by the partition function Z. For a binary mixture of N_e electrons and N_i protons, Z is conveniently written as

$$Z(N_e,N_i,V,\beta) = Q(N_e,N_i,\beta)/N_e!N_i!, \qquad Q(N_e,N_i,\beta) = \sum_\sigma \int_V dq\,dr\,\rho(q,r,\sigma;\beta). \quad (1)$$

Here, $q \equiv \{\mathbf{q}_1,\mathbf{q}_2,...,\mathbf{q}_{N_i}\}$ comprises the coordinates of the protons, and $\sigma = \{\sigma_1,...,\sigma_{N_e}\}$ and $r \equiv \{\mathbf{r}_1,...,\mathbf{r}_{N_e}\}$ the electron spins and coordinates, respectively. The density matrix ρ in Eq. (1) is represented in standard way by a path integral [5]

$$\rho(q,r,\sigma;\beta) = \frac{1}{\lambda_i^{3N_i}\lambda_\Delta^{3N_e}} \sum_P (\pm 1)^{\kappa_P} \int_V dr^{(1)}\dots dr^{(n)} \times$$

$$\times\rho\left(q,r,r^{(1)};\Delta\beta\right)\dots\rho\left(q,r^{(n)},\hat{P}r^{(n+1)};\Delta\beta\right)\mathcal{S}(\sigma,\hat{P}\sigma'), \quad (2)$$

[1)] Mercator guest professor at Rostock University.

where $\Delta\beta \equiv \beta/(n+1)$ and $\lambda_\Delta^2 = 2\pi\hbar^2\Delta\beta/m_e$. Further, $r^{(n+1)} \equiv r$ and $\sigma' = \sigma$ i.e. the particles are represented by fermionic loops with the coordinates (beads) $[r] \equiv [r, r^{(1)}, \ldots, r^{(n)}, r]$. The electron spin gives rise to the spin part of the density matrix $\mathcal{S}$, whereas exchange effects are accounted for by the permutation operator $\hat{P}$ and the sum over the permutations with parity κ_P. Following Refs. [3, 6, 7] , we use a modified representation (3) of the high-temperature density matrices on the r.h.s. of Eq. (2) which is suitable for efficient direct fermionic PIMC simulations of plasmas. With the error of order $\epsilon \sim (\beta Ry)^2\chi/(n+1)$ vanishing with growing number of beads we obtain approximation

$$\sum_\sigma \rho(q, r, \sigma; \beta) = \frac{1}{\lambda_i^{3N_i}\lambda_\Delta^{3N_e}} \sum_{s=0}^{N_e} \rho_s(q, [r], \beta),$$

$$\rho_s(q, [r], \beta) = \frac{C_{N_e}^s}{2^{N_e}} \exp\{-\beta U(q, [r], \beta)\} \prod_{l=1}^{n} \prod_{p=1}^{N_e} \phi_{pp}^l \det|\psi_{ab}^{n,1}|_s, \tag{3}$$

$$U(q, [r], \beta) = U^i(q) + \sum_{l=0}^{n} \frac{U_l^e([r], \beta) + U_l^{ei}(q, [r], \beta)}{n+1},$$

where U^i, U_l^e and U_l^{ei} denote the sum of the binary interaction Kelbg potentials Refs. [8] Φ^{ab} between protons, electrons at vertex "l" and electrons (vertex "l") and protons, respectively.

In Eq. (3), $\phi_{pp}^l \equiv \exp[-\pi|\xi_p^{(l)}|^2]$ arises from the kinetic energy density matrix ρ^K of the electron with index p, and we introduced dimensionless distances between neighboring vertices on the loop, $\xi^{(1)}, \ldots, \xi^{(n)}$. Thus, explicitly, $[r] \equiv [r; r + \lambda_\Delta\xi^{(1)}; r + \lambda_\Delta(\xi^{(1)} + \xi^{(2)}); \ldots]$. The exchange matrix is given by

$$||\psi_{ab}^{n,1}||_s \equiv \left|\left|\exp\left\{-\frac{\pi}{\lambda_\Delta^2}|(r_a - r_b) + y_a^n|^2\right\}\right|\right|_s, \quad y_a^n = \lambda_\Delta \sum_{k=1}^{n} \xi_a^{(k)}. \tag{4}$$

As a result of the spin summation, the matrix carries a subscript s denoting the number of electrons having the same spin projection.

As example we present the equation of state, $\beta p = \partial \ln Q/\partial V = [\alpha/3V\partial \ln Q/\partial\alpha]_{\alpha=1}$,

$$\frac{\beta pV}{N_e + N_i} = 1 + \frac{(3Q)^{-1}}{N_e + N_i} \sum_{s=0}^{N_e} \int dq\, dr\, d\xi\, \rho_s(q, [r], \beta) \times$$

$$\times \left\{ \sum_{p<t}^{N_i} \frac{\beta e^2}{|q_{pt}|} - \sum_{p<t}^{N_e} |r_{pt}| \frac{\partial\Delta\beta\Phi^{ee}}{\partial|r_{pt}|} - \sum_{p=1}^{N_i}\sum_{t=1}^{N_e} |x_{pt}| \frac{\partial\Delta\beta\Phi^{ie}}{\partial|x_{pt}|} - \right.$$

$$\left. - \sum_{l=1}^{n} \left[\sum_{p<t}^{N_e} A_{pt}^l \frac{\partial\Delta\beta\Phi^{ee}}{\partial|r_{pt}^l|} + \sum_{p=1}^{N_i}\sum_{t=1}^{N_e} B_{pt}^l \frac{\partial\Delta\beta\Phi^{ie}}{\partial|x_{pt}^l|} \right] + \frac{\alpha}{\det|\psi_{ab}^{n,1}|_s} \frac{\partial \det|\psi_{ab}^{n,1}|_s}{\partial\alpha} \right\}, \tag{5}$$

$$A_{pt}^l = \frac{\langle r_{pt}^l | r_{pt}\rangle}{|r_{pt}^l|}, \qquad B_{pt}^l = \frac{\langle x_{pt}^l | x_{pt}\rangle}{|x_{pt}^l|}.$$

Here, α is a length scaling, $\alpha = L/L_0$, $\langle \ldots | \ldots \rangle$ denotes the scalar product, and q_{pt}, r_{pt} and x_{pt} are differences of two coordinate vectors: $q_{pt} \equiv q_p - q_t$, $r_{pt} \equiv r_p - r_t$, $x_{pt} \equiv r_p - q_t$, $r_{pt}^l = r_{pt} + y_{pt}^l$, $x_{pt}^l \equiv x_{pt} + y_p^l$ and $y_{pt}^l \equiv y_p^l - y_t^l$. Other thermodynamic quantities exhibit the analogous form.

We demonstrate our numerical scheme for a two-component electron-proton plasma. In the simulations we used $N_e = N_p = 50$. To test the MC procedure we first consider a mixture of *ideal* electrons and protons for which the thermodynamic quantities are known analytically, e.g. [9]. Fig.1 shows our numerical results for the pressure together with the theoretical curve. The agreement, up to values of the degeneracy parameter χ as large

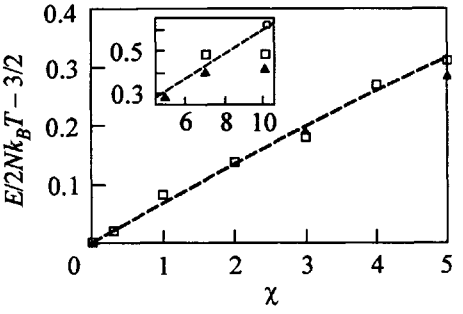

Fig.1. Energy E of an *ideal* plasma of degenerate electrons and classical protons in excess to the classical energy. PIMC simulation results with varying particle number are shown: $N = 32$ (triangles), $N = 50$ (squares) and $N = 90$ (circles) are compared to the exact analytical result (dashed line)

as 10 is evident and improves with increasing particle number. This clearly proofs that our method correctly samples the fermionic permutations. Note that for fast generation of a MC sequence of N-particle configurations it is necessary to efficiently compute the acceptance probability of new configurations, which is proportional to the absolute value of the ratio of the exchange determinants of two subsequent configurations, while the sign of the determinants is included into the weight function of each configuration.

Let us now turn to the case of *interacting* electrons and protons. We have performed a series of calculations in which the classical coupling parameter Γ was kept constant while the degeneracy parameter χ was varied, cf. Fig.2. One can see that, for weak coupling (cf. $\Gamma = 0.4$) and small degeneracy parameters, $\chi < 0.5$, there is good agreement

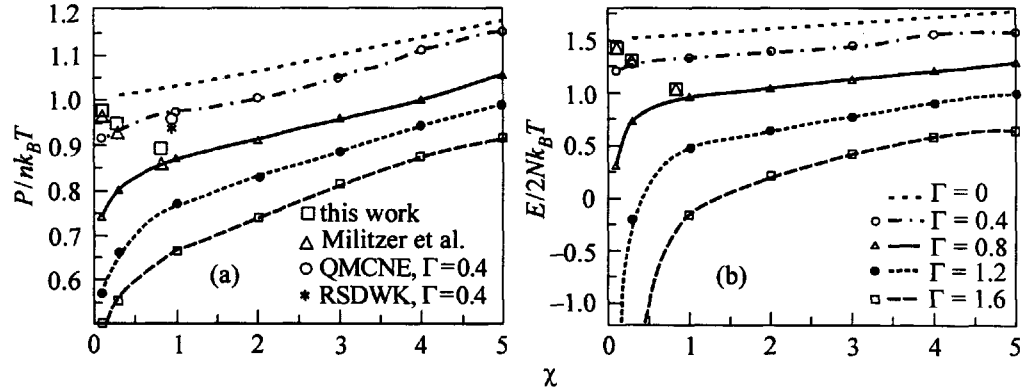

Fig.2. Pressure P (a) and energy E (b) of the *nonideal* plasma as a function of the quantum parameter χ. Curves correspond to different values of the coupling parameter Γ given in the inset of the lower figure. Large circle denotes quantum MC simulations without exchange (QMCNE) and large asterisk, the weak coupling model of Riemann et al. (RSDWK), data from [10]. The large triangles are recent restricted PIMC results of Militzer et al. [11] which are compared to our results (large squares) for three values of Γ – from top to bottom: $\Gamma = 0.169, 0.338, 0.672$

with analytical theories and quantum MC simulations without exchange [10]. However, as expected, with increasing χ and Γ, the deviations are growing rapidly. This figure

also contains comparison with restricted path integral results of Militzer et al. [11] (cf. the large triangles) corresponding to values of the coupling parameter in the range of $0.17, \ldots, 0.672$. Evidently, the agreement, in particular, of the energies is very good. The deviations in the pressure are apparently related to the fixed nodes approximation used in Ref. [11] and need further investigation.

A very interesting result is that the energy curves in Fig.2 become almost parallel as the degeneracy increases. In contrast, for $\Gamma > 0.6$ reduction of χ leads to a rapid decrease of the energy which is due to the formation of atoms and molecules as will be shown below.

The main advantage of the presented method is that it allows to investigate dense plasmas in a variety of physical situations which are very difficult to describe reliably by other approaches. This includes partial ionization and dissociation, Mott effect and ionic ordering at high densities. To investigate these phenomena, we show in Fig.3 the pair distribution functions for the four most interesting physical situations. Fig.3a clearly shows the

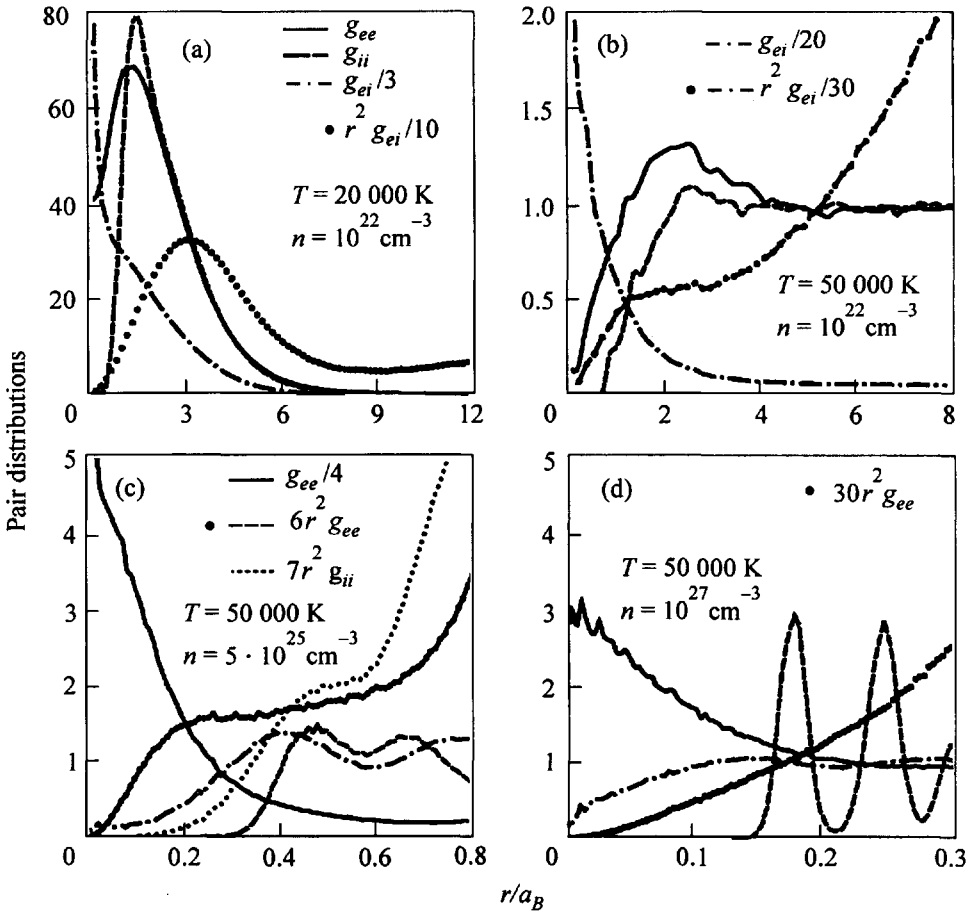

Fig.3. Electron-electron (g_{ee}, full line), ion-ion (g_{ii}, dashed line) and electron-ion (g_{ei}, dash-dotted line) pair distribution functions for dense hydrogen. The line styles in figs.b, c are the same as in fig. a. Notice the varying scalings of the curves. The values for the coupling, degeneracy and Brueckner parameters are: (a) $\Gamma = 2.9$, $\chi = 1.46$, $r_s = 5.44$; (b) $\Gamma = 1.16$, $\chi = 0.37$, $r_s = 5.44$; (c) $\Gamma = 19.8$, $\chi = 1848$, $r_s = 0.318$; and (d) $\Gamma = 53.8$, $\chi = 37.000$, $r_s = 0.117$

existence of hydrogen molecules (cf. the peaks of the proton-proton and electron-electron pair distribution functions at a separation of about $1.4a_B$) and atoms. We mention that the peak of the electron-proton function (multiplied on r^2) in our calculations appears at $r = 1a_B$ if no molecules are present (e.g. at lower density). But for the situation of Fig.3a, the presence of molecules leads to a shift of the peak to larger distances. Fig.3b shows that, with increasing temperature, atoms and molecules breakup which is clearly seen by the drastic lowering of the mentioned peaks of the pair distribution functions.

Let us now consider the case of higher densities while keeping the temperature constant. Here, our calculations predict interesting physical phenomena. In Figs.3b-d one clearly sees increased ordering of protons from a partially ionized plasma (3b, $\Gamma \approx 1.2$) over liquid-like (3c, $\Gamma \approx 20$) to solid-like (3d, $\Gamma \approx 54$) behavior, cf. the proton-proton pair distribution functions.

Notice further the qualitative change of the electron-electron function during the density increase from Fig.3b to 3d: g_{ee} in Fig.3b is typical for partially ionized plasmas, whereas in Fig.3c, a strong peak at low distances is observed. Further increase of the density leads to an almost uniform electron distribution in Fig.3d. To better understand the electron behavior, we included in Fig.3c the functions $r^2 g_{ee}$ and $r^2 g_{ii}$ also. The shoulders of these functions indicate that the most probable inter-electronic distance is almost two times smaller than the average distance between two protons. The reason of ths behavior in Fig.3c is *pairing of electrons* with opposite spin projection. The analysis of the electronic beads distribution allows us to conclude that the "extension" of the electrons is of the order of the inter-ionic distance, and that there is partial overlap of individual electrons. Under these conditions, pairing of (part of) the electrons minimizes the total energy of the system. This effect vanishes with increasing density due to the growing wave function overlap.

This work is supported by the Deutsche Forschungsgemeinschaft (Mercator-Programm) and the NIC Jülich. We acknowledge stimulating discussions with W.Ebeling, D.Kremp, W.D.Kraeft, M.Schlanges and thank B.Militzer for providing the data of Ref. [11].

---

1. See e.g. the papers of H.E.DeWitt et al., W.Ebeling et al. and D.Klakow et al. in *Proc. of the Intern. Conf. on Strongly Coupled Plasmas*, Eds. W.D.Kraeft and M.Schlanges, World Scientific, Singapore 1996.
2. Cf. for example the recent reviews of C.Shumway et al., J.P.Hansen et al. and Ya.Rosenberg, in *Proc. of the Intern. Conf. on Strongly Coupled Coulomb Systems*, Staint Malo, France, 1999; J.de Phys. IV **10**, Pr.5 (2000).
3. V.M.Zamalin, G.E.Norman, and V.S.Filinov, *The Monte Carlo Method in Statistical Thermodynamics*, Nauka, Moscow, 1977.
4. D.Ceperley, *The Monte Carlo and Molecular Dynamics of Condensed Matter Systems*, Eds. K.Binder and G.Cicotti, SIF, Bologna, 1996.
5. R.P.Feynman and A.R.Hibbs, *Quantum mechanics and path integrals*, McGraw-Hill, New York, 1965.
6. V.S.Filinov, High Temperature **13**, 1065 (1975); **14**, 225 (1976).
7. B.V.Zelener, G.E.Norman, and V.S.Filinov, High Temperature **13**, 650 (1975).
8. G.Kelbg, Ann. Physik **12**, 219 (1963); **13**, 354 (1963); **14**, 394 (1964); W. Ebeling, H.J. Hoffmann, and G. Kelbg, Beitr. Plasmaphys. **7**, 233 (1967) and references therein.
9. W.D.Kraeft, D.Kremp, W.Ebeling, and G.Röpke, *Quantum Statistics of Charged Particle Systems*, Akademie-Verlag, Berlin, 1986 (Russian translation, Mir, Moscow, 1988).
10. J.Riemann, M.Schlanges, H.E.DeWitt, and W.D.Kraeft, in Ref. [1], p.82.
11. B.Militzer and D.Ceperley, submitted to Phys. Rev. Lett.